

DOI:10.7522/j.issn.1000-0240.2023.0068

YAN Xuchun, WU Xiaodong, LÜ Yaqiong, et al. Applicability evaluation of CLM5.0 in simulating soil temperature and carbon cycle in Alaskan permafrost region[J]. Journal of Glaciology and Geocryology, 2023, 45(3):902-914. [闫旭春, 吴晓东, 吕雅琼, 等. CLM5.0对阿拉斯加多年冻土区土壤温度和碳循环模拟的适用性评估[J]. 冰川冻土, 2023, 45(3):902-914.]

# CLM5.0对阿拉斯加多年冻土区土壤温度和碳循环模拟的适用性评估

闫旭春<sup>1,2</sup>, 吴晓东<sup>1</sup>, 吕雅琼<sup>3</sup>, 吴通华<sup>1</sup>, 李 韧<sup>1</sup>, 胡国杰<sup>1</sup>,  
邹德富<sup>1</sup>, 刘亚东<sup>1,2</sup>, 魏献花<sup>1,2</sup>, 范晓英<sup>1,2</sup>, 王 栋<sup>1,2</sup>

(1. 中国科学院 西北生态环境资源研究院 冰冻圈科学国家重点实验室 藏北高原冰冻圈特殊环境与灾害国家野外科学观测研究站, 甘肃 兰州 730000; 2. 中国科学院大学, 北京 100049; 3. 中国科学院、水利部 成都山地灾害与环境研究所, 四川 成都 610299)

**摘 要:** 气候变暖对北极多年冻土和植被产生了重要的影响。CLM(Community Land Model)是应用最广泛的陆面过程模式之一,但其中复杂的边界条件和参数化过程导致模式模拟结果存在一定的不确定性。本研究评估了CLM5.0对阿拉斯加多年冻土区表层土壤温度和碳循环的模拟能力,结果表明,CLM5.0可以捕捉到表层土壤温度的季节变化。在苔原和针叶林站点,CLM5.0在日尺度和月尺度都可以很好地模拟出总初级生产力(GPP)随时间的变化,但对净生态系统碳交换(NEE)的模拟结果存在一定的不确定性。CLM5.0可以较为合理地模拟高纬度多年冻土区的土壤温度季节变化,在未来的研究中可能还需要从结构、参数化方案等过程进行改进,从而进一步提升高纬度多年冻土区碳循环的模拟精度。

**关键词:** CLM5.0; 阿拉斯加; 土壤温度; 碳循环; 多年冻土

**中图分类号:** P642.14; S154.1 **文献标志码:** A **文章编号:** 1000-0240(2023)03-0902-13

## 0 引言

多年冻土约占北半球陆地表面的22%<sup>[1]</sup>,是最大的陆地土壤碳库,其碳储量是大气的两倍<sup>[2-5]</sup>。在过去的几十年中,北极经历了快速的变暖<sup>[6]</sup>,大多数多年冻土地区加速退化<sup>[7]</sup>。多年冻土退化会引起低温环境中的土壤有机质分解,释放出大量的温室气体进入空气中,从而对气候变暖产生正反馈<sup>[3,8]</sup>。

北极地区的气候变化影响其植被的组成。随着夏季气温的升高,禾本科和矮灌木丛的数量增加<sup>[9]</sup>,而苔藓和地衣的物种多样性呈下降趋势<sup>[10]</sup>。来自卫星观测数据证明北半球高纬度地区正在变绿<sup>[11]</sup>,灌木的扩张正在改变北半球高纬度的植物群落组成<sup>[12]</sup>和生态系统碳平衡<sup>[13]</sup>。

气候变暖可能使高纬度地区多年冻土生态系

统在21世纪末从碳汇转变为碳源<sup>[14]</sup>。基于过程模型、大气反演模型等,北极苔原在过去几十年是CO<sub>2</sub>的汇和CH<sub>4</sub>的源<sup>[15]</sup>。基于CanESM2及ISI-MIP,北半球中高纬度陆地生态系统在未来仍然是碳汇<sup>[16-17]</sup>。然而,陆面过程模式中复杂的边界条件和参数化过程,导致模式存在一定的不确定性。因此,为了提升模式结果的可靠性,扩大其应用范围,促进陆面模式发展,进行模式性能的适用性评估是十分必要的。

Community Land Model version 5.0(CLM5.0)是Community Earth System Mode version 2.0的陆面模块最新版本<sup>[18]</sup>。CLM是应用最广泛的陆面过程模式之一,并且有助于全球模式的比较和对于未来气候的预测<sup>[17,19]</sup>。CLM可以模拟出北半球多年

收稿日期: 2022-08-28; 修订日期: 2022-11-14

基金项目: 国家自然科学基金项目(41941015;32061143032;41871060);中国科学院“西部之光”人才培养计划项目资助

作者简介: 闫旭春,硕士研究生,主要从事北半球高纬度地区陆地植被和生态系统碳库变化研究. E-mail: yanxuchun@nieer.ac.cn

通信作者: 吴晓东,研究员,主要从事多年冻土与环境研究. E-mail: wuxd@lzb.ac.cn

冻土区冻土的变化趋势<sup>[20]</sup>和未来变暖情景下的碳动态<sup>[21]</sup>。目前最新版本的CLM5.0对于与植被相关的碳通量、水通量、能量通量和生物地球化学进行了改进<sup>[22]</sup>。与过去版本的模型(即CLM4.0和CLM4.5)相比,CLM5.0在全球范围内都有所改善。已经在全球很多区域对CLM碳循环的模拟性能进行了评估,强迫数据、植被功能型、植物氮循环、微生物动态和积雪方案等的改进可以降低CLM碳循环模拟的偏差<sup>[21,23-27]</sup>。

在本研究中,选择了阿拉斯加多年冻土区两种地表覆盖类型(苔原和常绿针叶林)三个观测站点的实测数据对CLM5.0在高纬度多年冻土区的土壤温度和碳循环的模拟性能进行评估分析。研究结果有助于更好地理解北极地区的植被生长和碳循环对于气候变化的响应。

1 数据与方法

1.1 研究区概况

阿拉斯加位于北半球高纬度地区(图1),经纬

度范围54°~71°N、130°~173°W。三面环海(北太平洋、白令海和北冰洋),降水量丰富(多积雪)。多年冻土约占阿拉斯加总面积的80%,包括连续多年冻土(29%)、不连续多年冻土(35%)、零星多年冻土(8%)和岛状多年冻土(8%)。阿拉斯加15%的地区没有多年冻土,冰川和冰盖占总面积的4%,大型水体占总面积的1%<sup>[28]</sup>,主要地表覆盖类型为苔原和森林<sup>[29]</sup>。选择三个站点为研究对象 Atqasuk (US\_Atq)<sup>[30]</sup>、Ivotuk (US\_Ivo)<sup>[31]</sup>、Poker Flat Research Range Black Spruce Forest (US\_Prr)<sup>[32]</sup>。US\_Atq 站点位于阿拉斯加 Barrow 南 100 km 连续多年冻土区,为排水良好的高地,植被类型为苔原(潮湿沿海莎草),站点年均积雪覆盖 300 天;US\_Ivo 站点位于阿拉斯加 Barrow 南 300 km 布鲁克斯山脉山麓的连续多年冻土区,植被类型为苔原(矮灌木、苔藓),站点年均积雪覆盖 280 天;US\_Prr 站点位于阿拉斯加中部不连续多年冻土区,地形平坦,植被类型为常绿针叶林(黑云杉林),站点年均积雪覆盖 210 天。详细信息如表1所示。

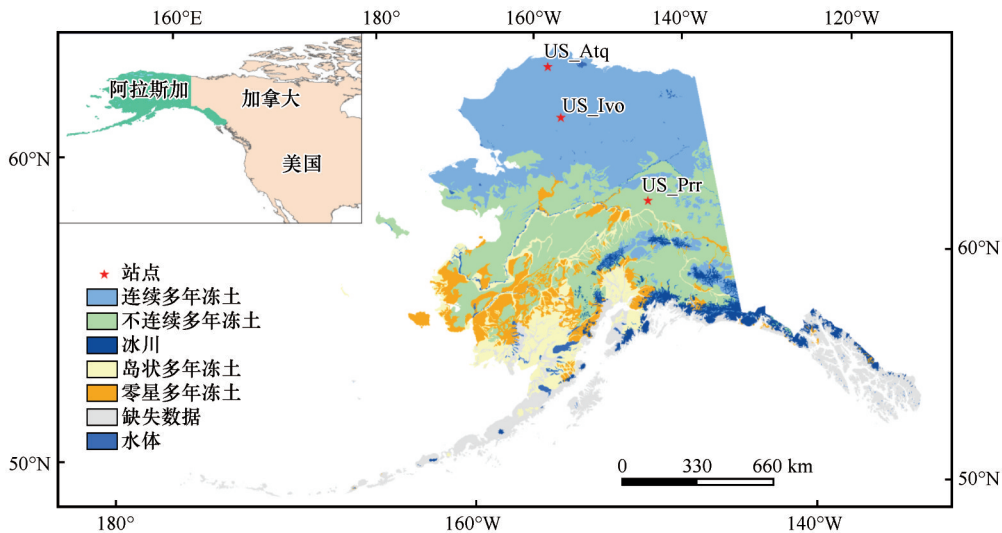


图1 阿拉斯加观测站点位置  
Fig. 1 Location of the observation sites in Alaska

表1 阿拉斯加研究站点信息  
Table 1 Information of the observation sites in Alaska

站点	观测时间	植被类型	经纬度	海拔/m	年平均降水量/mm	年平均气温/℃
US_Atq	2004—2008年	苔原	157.409°W, 70.470°N	15	93	-9.70
US_Prr	2011—2013年	针叶林	147.488°W, 65.124°N	210	275	-2.00
US_Ivo	2005—2006年	苔原	155.750°W, 68.487°N	568	304	-8.28

注: US\_Atq、US\_Prr 和 US\_Ivo 站点年平均降水量和年平均气温数据的年份分别为 1999—2008 年、2011—2016 年和 2003—2016 年。

1.2 数据

CLM5.0 大气驱动数据来自 Fluxnet ([https://](https://fluxnet.org)

[fluxnet.org](https://fluxnet.org)) 和 Ameriflux (<https://ameriflux.lbl.gov>), 包括半小时时间分辨率的近地表气温、近地表气压、

相对湿度、降水、风速、向下长波和短波辐射。总初级生产力(gross primary productivity, GPP)和净生态系统碳交换(net ecosystem exchange, NEE)数据来自 FLUXNET2015<sup>[33]</sup>。表层土壤温度数据来自 Fluxnet。模型强迫数据质量控制,包括异常值的去除和缺失数据插补(缺失数据小于2小时用线性内插法,大于2小时用回归法)。

### 1.3 模型描述

CLM5.0 广泛应用于模拟陆地生态系统中的水、能量和碳氮通量<sup>[34]</sup>。CLM5.0 是 CESM2.0 的陆面模块的最新版本<sup>[22]</sup>。在 CLM5.0 中,模拟的地表通量(如潜热和感热)是由大气和气象输入变量驱动,同时结合了土壤、植被的状态(如土壤湿度和叶面积指数)和参数(如导水率和地表覆盖)<sup>[35-36]</sup>。CLM5.0 在 CLM4.5 的基础上更新了大部分组分的过程和参数化,包括土壤结构、植被水文、积雪密度、碳氮循环和耦合、作物模型、土地利用等模块。同时考虑了网格尺度内地表特征差异、不同植被类型下生态学差异以及不同土壤类型水力学和热力学特征差异等。此外,该模型包括详尽的生物地球物理过程和生物地球化学过程<sup>[22]</sup>。水文方面的改进是在模型中引入了干表层的土壤蒸发阻力参数化方案,可以有效地改善半干旱地区土壤水分、蒸散发以及地下水的模拟精度<sup>[37]</sup>。土壤垂直层数增加到25层(20个土壤层和5个基岩层),主要增加了0~3 m的土壤层数,可以更好地模拟多年冻土区活动层厚度<sup>[22]</sup>。积雪密度方面考虑了风对新雪密度的影响,最大雪层数从5层增加到12层,雪水当量模拟增加到10 m<sup>[38]</sup>。植物生理方面将 Ball-Berry 气孔导度方案替换为 Medlyn 方案<sup>[39]</sup>。碳氮循环和耦合方面的主要改进是氮循环的碳成本方案(FUN)、可变植被碳氮比方案(FLEXIBLECN)和基于叶氮的光合同化方案(LUNA)<sup>[22,40-44]</sup>。同时,土壤碳分解过程中重新评估土壤碳周转的温度敏感性,使土壤碳分解速率随深度下降减弱<sup>[45]</sup>。

### 1.4 模型模拟实验设计

本研究使用 CLM5.0 生物地球化学模式(bio-geochemistry, CLM5.0-BGC)在阿拉斯加3个观测站进行了单点离线模拟试验,利用气象数据作为 CLM5.0 模式的强迫数据,为了使模式碳氮状态达到平衡,驱动模式进行200年预热(spin-up),并以平衡状态的初始场进行单点离线模拟分析。模型模拟过程中,以实测的地表数据替换了模型中每个站

点的默认值,包括砂土和黏土百分比含量,实测中缺失的土壤质地数据来自全球土壤数据 GS-DE<sup>[46]</sup>(表2)。

表2 观测站点的土壤质地信息

Table 2 Information of soil texture at the observation sites

深度/m	US_Atq		US_Prr		US_Ivo	
	黏粒/%	砂粒/%	黏粒/%	砂粒/%	黏粒/%	砂粒/%
0.01	30	54	7	34	17	36
0.04	30	54	7	34	17	36
0.09	16	40	7	34	17	38
0.16	16	39	6	35	16	40
0.26	16	39	5	36	17	37
0.40	17	33	5	40	17	37
0.58	14	38	5	40	17	35
0.80	14	38	4	50	15	35
1.05	20	27	4	50	15	35
1.36	20	27	23	43	18	39

### 1.5 评价指标

本文将模拟和观测数据处理为日平均值和月平均值。为了量化模拟和观测之间的差异,在每个站点计算了四个统计特征:决定系数( $R^2$ )、均方根误差(RMSE)、平均绝对误差(MAE)和平均偏差(MBE)。具体计算公式为

$$R^2 = \frac{\sum_{i=1}^N (M_i - O_i)^2}{\sum_{i=1}^N (O_i - \bar{O})^2} \quad (1)$$

$$\text{RMSE} = \sqrt{\frac{1}{N-1} \sum_{i=1}^N (M_i - O_i)^2} \quad (2)$$

$$\text{MAE} = \frac{1}{N} \left| \sum_{i=1}^N (M_i - O_i) \right| \quad (3)$$

$$\text{MBE} = \frac{1}{N} \sum_{i=1}^N (M_i - O_i) \quad (4)$$

式中: $N$ 为时间长度; $M_i$ ( $i=1, 2, \dots, N$ )为模拟值; $O_i$ 为实测值; $\bar{O}$ 为实测值的平均值。

## 2 结果

### 2.1 表层土壤温度模拟

CLM5.0 可以较好地模拟出表层土壤温度(2 cm 和 5 cm)的季节变化,在 US\_Atq 站点(植被类型为苔原)对表层土壤温度(2 cm 和 5 cm)的结果优于 US\_Prr(植被类型为针叶林)(图2)。其他统计数据也表明 CLM5.0 对于 US\_Atq 站点表层土壤温度(2 cm 和 5 cm)的模拟结果更好(表3)。US\_Atq 站点对表层土壤温度的模拟在冬季和早春普遍低估;

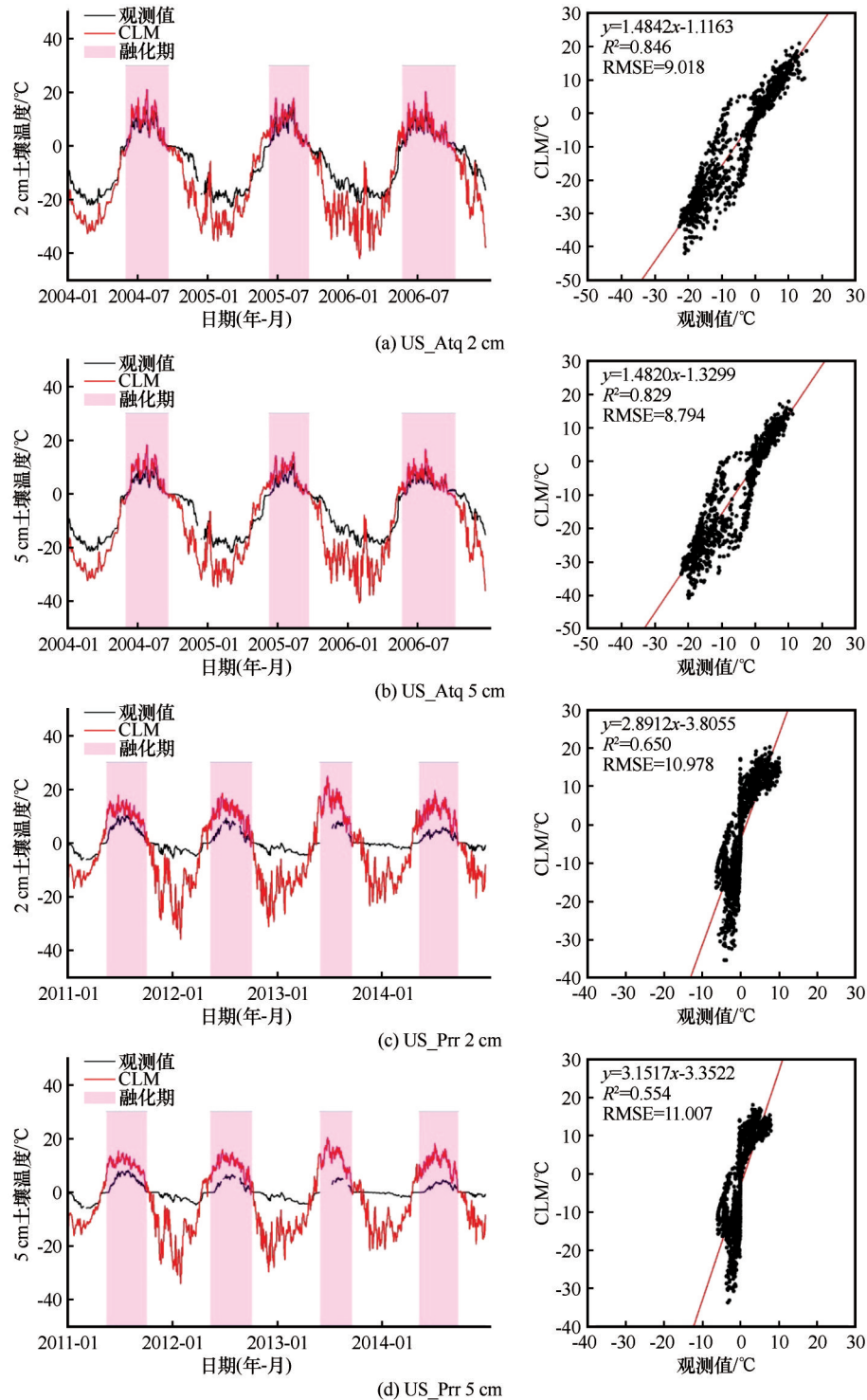


图2 站点模拟和观测的表层土壤温度[左图为模型模拟(红色线)和观测(黑色线)的表层土壤温度时间序列;右图为模拟和观测的散点图,红色直线为拟合线。其中,阴影表示融化期(使用2 cm深度土壤温度高于或低于0 °C,来确定融化期的开始和结束日期<sup>[47]</sup>)。US\_Atq融化期为2004年151—264日(积日,下同),2005年161—267日,2006年144—285日;US\_Prr融化期为2011年135—277日,2012年133—279日,2013年150—264日,2014年132—270日]

Fig. 2 Simulated and observed surface soil temperature [The left panels show time series of CLM simulations (red lines) and observed surface soil temperature (black lines); the right panels show scatter plots of CLM simulations and observed surface soil temperature, and the red lines are fitted lines. In this study, shading indicates the thawing period (The thaw start-date, thaw end-date, and thaw duration were calculated by determining daily soil temperature at a depth of 2 cm was above or below 0 °C<sup>[47]</sup>). The thawing period is from 151 to 264 (day of year, the same below) in 2004, 161 to 267 in 2005, 144 to 285 in 2006 at US\_Atq site; from 135 to 277 in 2011, 133 to 279 in 2012, 150 to 264 in 2013, 132 to 270 in 2014 at US\_Prr site]



表3 各站点模拟表层土壤温度的评价指标  
Table 3 Evaluation indexes of simulated soil temperature  
at the observation sites

站点及土层	季节	$R^2$	RMSE/℃	MAE/℃	MBE/℃
US_Atq 2 cm 土壤温度	全年	0.846	9.018	7.062	-4.042
	春季	0.860	6.541	5.506	1.508
	夏季	0.778	3.464	2.649	1.964
	秋季	0.740	10.494	8.627	-8.627
	冬季	0.573	12.759	11.582	-11.377
US_Atq 5 cm 土壤温度	全年	0.829	8.794	6.773	-4.343
	春季	0.838	5.985	4.935	0.772
	夏季	0.809	2.607	2.029	1.620
	秋季	0.724	10.464	8.687	-8.687
	冬季	0.534	12.660	11.602	-11.478
US_Prr 2 cm 土壤温度	全年	0.650	10.978	9.065	-3.439
	春季	0.792	7.132	6.165	3.392
	夏季	0.493	7.351	6.727	6.718
	秋季	0.674	12.260	9.531	-8.684
	冬季	0.049	14.709	13.489	-13.489
US_Prr 5 cm 土壤温度	全年	0.554	11.007	9.121	-3.417
	春季	0.814	6.855	5.901	3.035
	夏季	0.390	7.241	7.243	7.241
	秋季	0.567	12.229	9.456	-8.585
	冬季	0.013	14.758	13.575	-13.574

而US\_Prr站点表层土壤温度的模拟在冬季和早春存在普遍低估,在夏季存在普遍的高估。整体而言,CLM5.0对于苔原植被的土壤温度的模拟结果与针叶林植被的模拟结果相比RMSE、MAE平均降低约2℃。

## 2.2 GPP与NEE模拟

CLM5.0可以模拟出各个站点GPP随时间的变化(图3)。CLM5.0对于GPP的模拟在生长季存在普遍的高估。该模型在US\_Atq站点的模拟更接近观测(表4)。在US\_Atq站点模拟的GPP相较于其他两个站点的模拟结果 $R^2$ 平均提高约0.1,MAE平均降低0.2 gC·m<sup>-2</sup>·d<sup>-1</sup>。CLM5.0可以捕捉到NEE在各个站点随时间的变化,但是对于NEE的模拟精度较低(图4,表4)。与观测数据相比,CLM5.0在US\_Atq和US\_Ivo站点对于NEE的模拟在冬季和早春表现出更强的碳吸收,在夏秋季表现出更强的碳释放;而US\_Prr站点对于NEE的模拟表现则相反,在夏秋季固碳能力更弱。

与日时间尺度的模拟结果相比,CLM5.0在月时间尺度上对GPP和NEE的模拟结果有所改善(图5~6,表5)。CLM5.0对GPP和NEE月尺度模拟的结

果显示,三个站点在生长季对GPP的模拟普遍高估,US\_Atq和US\_Ivo站点对于NEE的模拟在冬季和早春表现出更强的碳吸收,在夏秋季表现出更强的碳释放,而US\_Prr站点对于NEE的模拟表现则相反,夏秋季固碳能力更弱,这与日时间尺度的模拟趋势相同。

## 3 讨论

### 3.1 模型对表层土壤温度模拟精度的评估

CLM5.0可以很好地捕捉到表层土壤温度随时间变化的特征。但是对于冻结期,在阿拉斯加两个站点的模拟的土壤温度存在一定的“冷偏差”;而在融化期,对于表层土壤温度的模拟高估(MBE>0℃),存在“暖偏差”。目前大多数模式的结果都存在这种土壤温度的“冷偏差”<sup>[48-49]</sup>。通过改进冬季空气动力学阻抗可以有效改善土壤温度的“冷偏差”<sup>[50]</sup>。植被与多年冻土之间存在着复杂的相互作用。植被类型和覆盖模式的不同导致来自地表的热量和水分的传输效率的不同<sup>[51]</sup>,此外,植被覆盖差异也会导致土壤不同的冻融循环和多年冻土水热条件<sup>[52-53]</sup>。植被通过改变水-热耦合,影响多年冻土的变化<sup>[54]</sup>。为了探究不同植被类型对于土壤表层温度模拟偏差的影响,将US\_Prr站点的植被类型替换为苔原。研究发现植被类型会改变地表温度的模拟结果(图7)。CLM5.0对于改变植被类型的模拟结果与原始结果相比 $R^2$ 平均提高0.02, RMSE、MAE平均降低约0.25℃(表6)。植被类型可能并不是引起土壤温度模拟偏差的主要原因,积雪可能是阿拉斯加土壤表层温度模拟一个重要的影响因素。阿拉斯加多年冻土区冬季降雪每年持续9个月,积雪厚度大,覆盖范围广,但是模式模拟的积雪覆盖度和厚度与实际情况相差较大,这可能使得模型对于地表温度的模拟出现偏差<sup>[55-56]</sup>。对于冻结期表层土壤温度模拟的低估,可能是由于活动层中频繁的冻融循环的发生,冰-水相变需要更多的能量,而使土壤温度降低<sup>[48,57]</sup>。在多年冻土区,模型中土壤水热动态之间的相互作用以及植被变化对其的影响还需更精确的描述<sup>[58-59]</sup>;同时,土壤水热耦合与植被之间相互作用的数值函数需要进一步优化<sup>[51]</sup>。除了模式物理参数可能存在的不确定性以外,大气驱动数据的不确定性是影响模式碳水循环的另一重要因素。相较于默认的地表参数,利用替换后的土壤质地数据模拟表层土壤温度的误差有所下降,其RMSE平均下降约0.14℃。土壤水热传输耦合

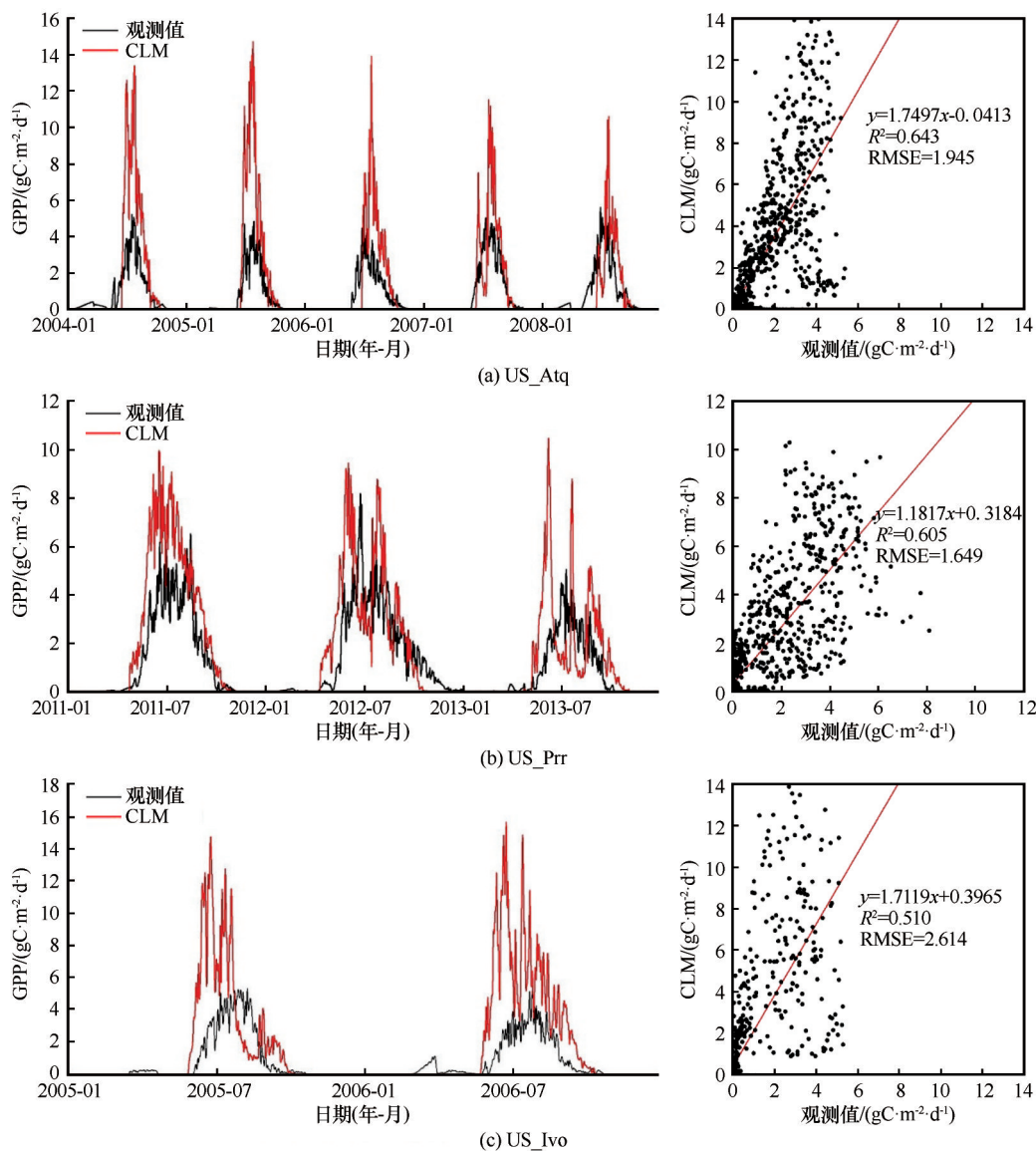


图3 日尺度模拟和观测的GPP [左图为模型模拟(红色线)和观测(黑色线)GPP的时间序列; 右图为模拟和观测的散点图,红色直线为拟合线]

Fig. 3 Simulated and observed GPP (gross primary production) on daily time scale [The left panels show time series of CLM simulations (red lines) and GPP using flux tower observations (black lines); the right panels show scatter plots of CLM simulations and observed GPP, and the red lines are fitted lines]

表4 各站点日尺度模拟GPP与NEE的评价指标

Table 4 Evaluation indexes of simulated GPP and NEE (net ecosystem exchange) on daily time scale at the observation sites

站点	模拟对象	$R^2$	RMSE/( $\text{gC}\cdot\text{m}^{-2}\cdot\text{d}^{-1}$ )	MAE/( $\text{gC}\cdot\text{m}^{-2}\cdot\text{d}^{-1}$ )	MBE/( $\text{gC}\cdot\text{m}^{-2}\cdot\text{d}^{-1}$ )
US_Atq	GPP	0.643	1.945	0.881	0.532
	NEE	0.253	1.009	0.627	0.040
US_Prr	GPP	0.605	1.649	0.944	0.529
	NEE	0.145	1.474	0.900	0.747
US_Ivo	GPP	0.510	2.614	1.246	0.956
	NEE	0.186	1.221	0.708	0.040

等多参数方案加入到Noah-MP中,减少了表层土壤温度模拟产生的冷偏差,改进了模型对于表层土壤

温度的模拟<sup>[60]</sup>,将其加入到CLM模型中,对于高纬度地区表层土壤温度的模拟精度提升<sup>[61]</sup>。

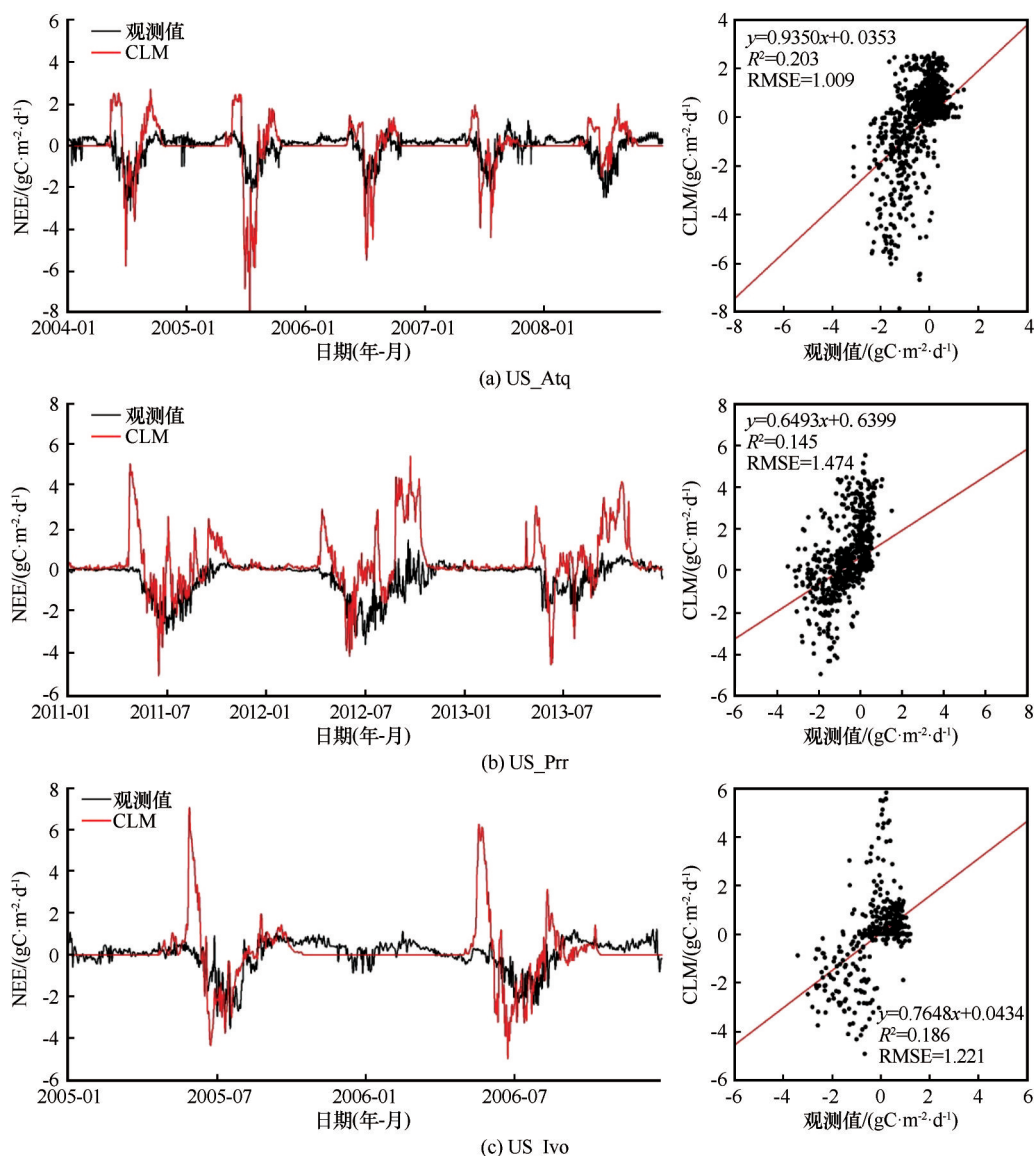


图4 日尺度模拟和观测的NEE [左图为模型模拟(红色线)和观测(黑色线)的NEE时间序列; 右图为模拟和观测的散点图,红色直线为拟合线]

Fig. 4 Simulated and observed NEE on daily time scale [The left panels show time series of CLM simulations (red lines) and NEE using flux tower observations (black lines); the right panels show scatter plots of CLM simulations and observed NEE, and the red lines are fitted lines]

### 3.2 模型对GPP与NEE模拟精度的评估

在阿拉斯加多年冻土区苔原和针叶林站点, CLM5.0在日尺度和月尺度都可以很好地模拟出GPP随时间的变化。同时,CLM也可以在其他研究区域捕捉到GPP随时间变化的趋势<sup>[21,26-27,62]</sup>。因此,CLM5.0可以用来在北极苔原和针叶林模拟GPP。CLM5.0虽然可以捕捉到NEE随时间的变化,但是其模拟结果有很大的不确定性,需要进一步对其参数化方案以及模型内在机理过程进行优化。另外,CLM5.0对于GPP和NEE的模拟表现出明显的季节特征(图5和图6)。在生长季期间,NEE为负值,

因为植被的生长可以增加碳吸收<sup>[63]</sup>。最大的碳吸收发生在7—8月,因为在这期间北极地区气温高和太阳辐射强。GPP的季节变化与植被生长的季节变化表现出很好的一致性。

在三个站点CLM5.0对于生长季GPP的模拟结果普遍高估,而对于NEE的模拟结果展现出很大的不确定性,可能是由于模型结构和参数化的不确定性导致的<sup>[64-65]</sup>。夏季较高的气温和降水可能增加GPP模拟的不确定性。通过改变模型中植物的氮吸收方式,增加模型中积雪对地表的保温效果<sup>[21]</sup>,并且考虑模型中不同植被功能型的碳分配机制<sup>[27]</sup>,可



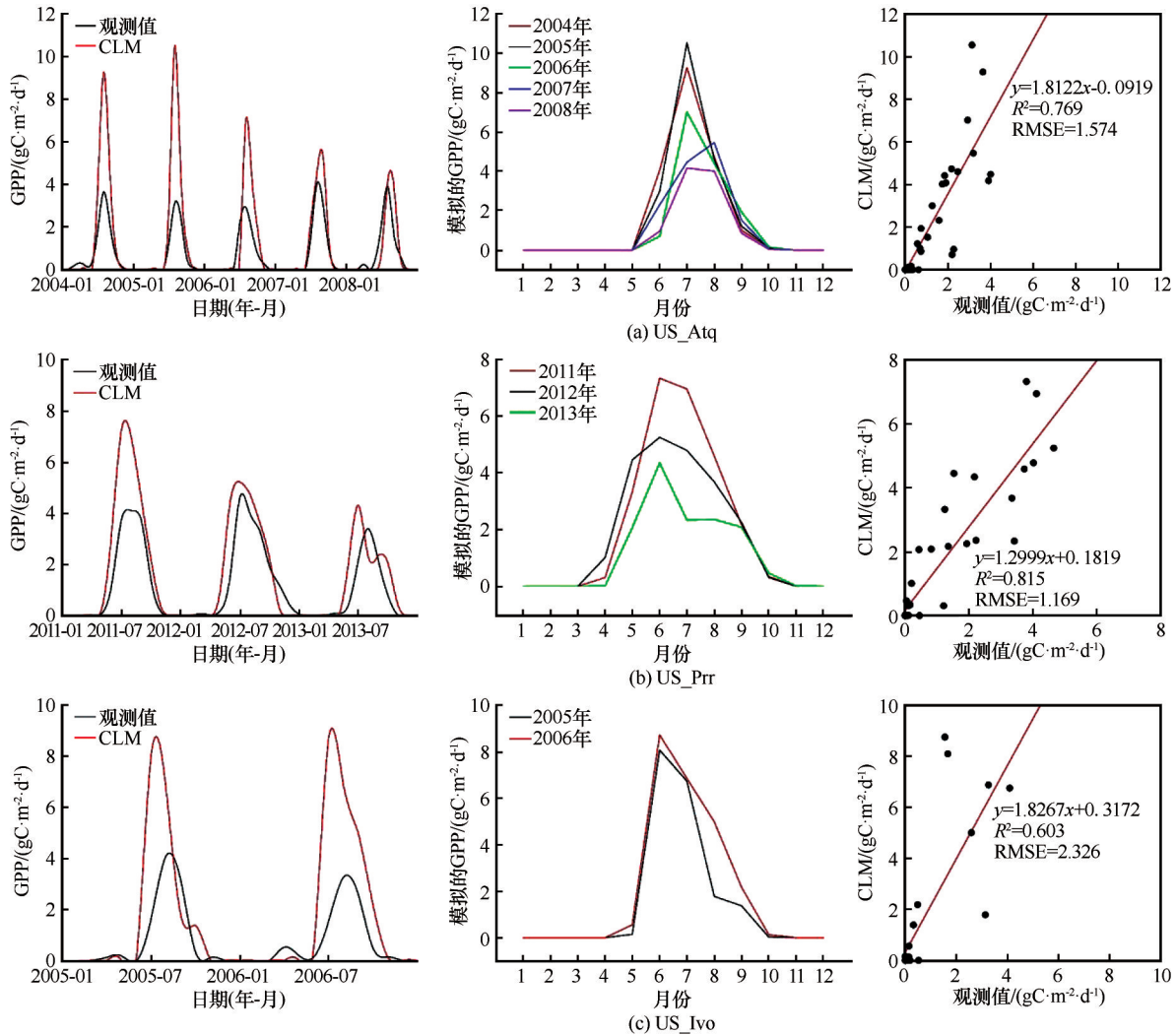


图5 月尺度模拟和观测的 GPP [左图为模型模拟(红色线)和观测(黑色线)GPP的时间序列;中间图为模型模拟的不同年份 GPP 月尺度变化;右图为模拟和观测的散点图,红色直线为拟合线]

Fig. 5 Simulated and observed GPP on monthly time scale [The left panels show time series of CLM simulations (red lines) and GPP using flux tower observations (black lines); the middle panels show monthly changes in simulated GPP for different years; the right panels show scatter plots of CLM simulations and observed GPP, and the red lines are fitted lines]

以有效减小 CLM 在 GPP 和 NEE 模拟方面的偏差。此外,强迫数据对于碳循环的影响也不可忽视<sup>[66]</sup>。

### 3.3 与其他模型对碳循环模拟结果的比较

在当前的气候条件下,在站点尺度,CLM5.0 对于阿拉斯加 NEE 的模拟表现出很强的碳吸收能力,同时也可以模拟出季节性 NEE 峰值时间。这与 ecosys 模型模拟结果以及基于观测的产品相一致,但是对于碳循环的季节性的捕捉还有很大的不确定性<sup>[67]</sup>。Fisher 等<sup>[68]</sup>用 10 个 North American Carbon Program (NACP) 站点集成模型比较分析了阿拉斯加 North Slope 苔原区域(Atkasuk 和 Barrow 站点)的 GPP 和 NEE。与本研究相比,在 US\_Atq 站点,CLM5.0 对于 NEE 模拟的  $R^2=0.407$ , 这比 10 个

NACP 站点集成模型的模拟结果更好( $R^2=0.13$ )。在 US\_Atq 站点观测到的最大的碳吸收通常是在 6 月,而 CLM5.0 模拟的最大碳吸收是在 7 月,CLM5.0 可以模拟出季节性 NEE 峰值时间,虽然模型模拟的 NEE 峰值有轻微时间滞后,但是也表明 CLM 可以扩展到区域分析,这与多模型平均的结果相一致<sup>[68]</sup>。

## 4 结论

本研究选取了阿拉斯加多年冻土区苔原和针叶林植被三个站点,评估了 CLM5.0 对于阿拉斯加多年冻土区对于表层土壤温度和碳循环的模拟性能。CLM5.0 可以较好地模拟出表层土壤温度



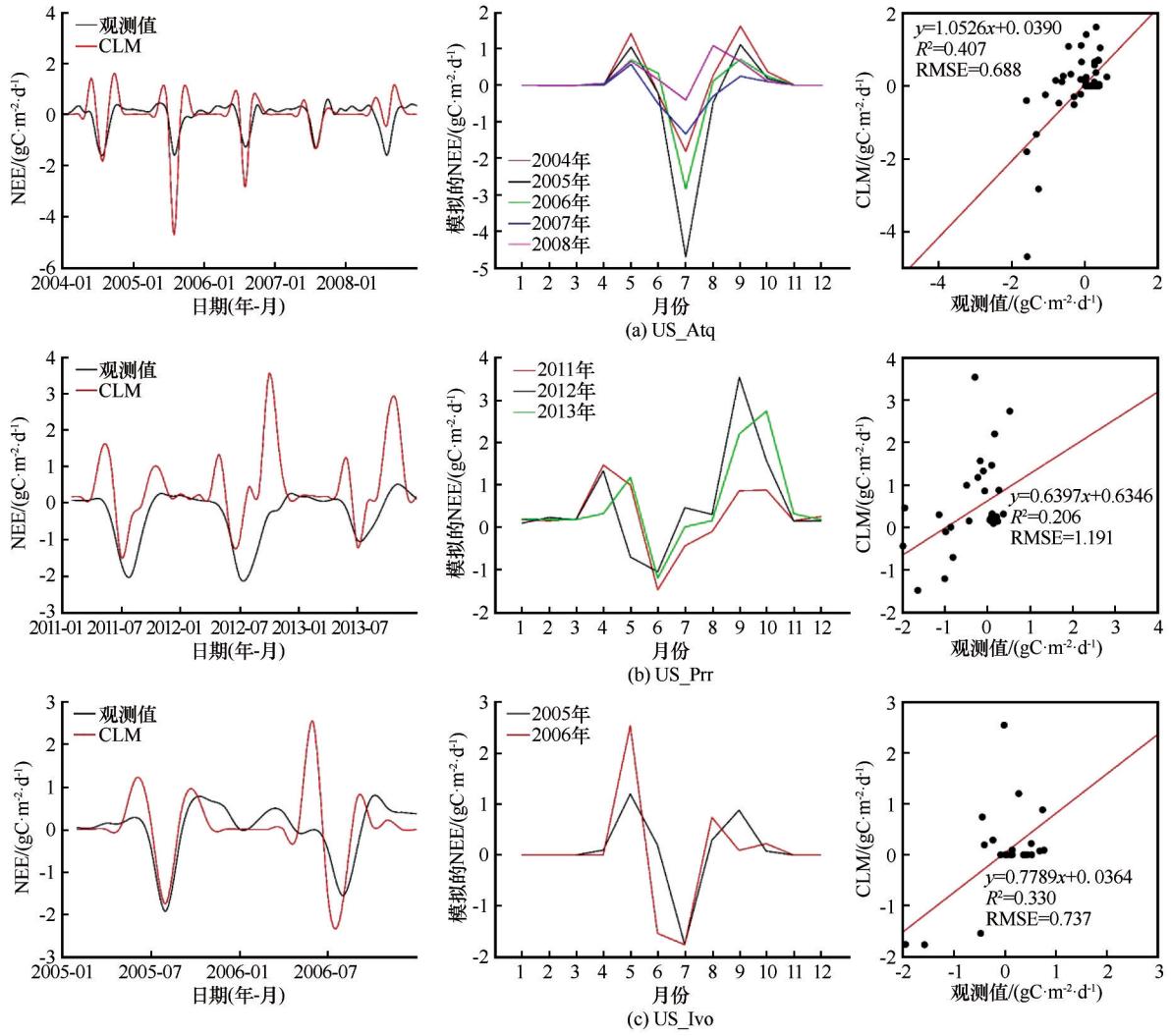


图6 月尺度模拟和观测的NEE [左图为模型模拟(红色线)和观测(黑色线)的NEE时间序列;中间图为模型模拟的不同年份NEE月尺度变化;右图为模拟和观测的散点图,红色直线为拟合线]

Fig. 6 Simulated and observed NEE on monthly time scale [The left panels show time series of CLM simulations (red lines) and NEE using flux tower observations (black lines); the middle panels show monthly changes in simulated NEE for different years; the right panels show scatter plots of CLM simulations and observed NEE, and the red lines are fitted lines]

表5 各站点月尺度GPP与NEE模拟的评价指标

Table 5 Evaluation indexes of simulated GPP and NEE on monthly time scale at the observation sites					
站点	模拟对象	$R^2$	RMSE/( $\text{gC}\cdot\text{m}^{-2}\cdot\text{d}^{-1}$ )	MAE/( $\text{gC}\cdot\text{m}^{-2}\cdot\text{d}^{-1}$ )	MBE/( $\text{gC}\cdot\text{m}^{-2}\cdot\text{d}^{-1}$ )
US_Atq	GPP	0.769	1.574	0.716	0.532
	NEE	0.407	0.688	0.448	0.037
US_Prr	GPP	0.815	1.169	0.704	0.542
	NEE	0.206	1.191	0.788	0.762
US_Ivo	GPP	0.603	2.326	1.218	0.999
	NEE	0.330	0.737	0.501	0.034

(2 cm和5 cm)的季节变化,对于苔原植被的土壤温度的模拟结果与针叶林植被的模拟结果相比RMSE、MAE平均降低约2℃。在冻结期,阿拉斯加两个站点的模拟的土壤温度存在一定的“冷偏差”;而在融化期,对于表层土壤温度的模拟存在“暖偏

差”,这可能是由于模型结构和参数化的不确定性导致的。土壤结构和大气强迫数据对模拟结果影响很大。与默认的地表参数相比,利用替换后的土壤质地数据模拟表层土壤温度的误差有所下降,其RMSE平均下降约0.14℃。在阿拉斯加多年冻土

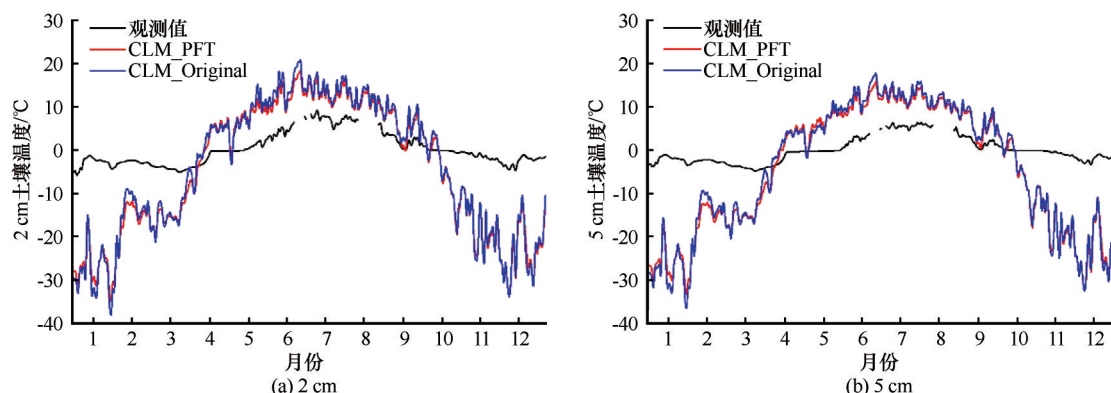


图7 US\_Prr 站点模拟和观测的表层土壤温度 [模型模拟 (CLM\_PFT 表示改变地表植被, 红色线; CLM\_Original 表示模型默认, 蓝色线) 和观测 (黑色线) 的表层土壤温度时间序列]

Fig. 7 Simulated and observed surface soil temperature at US\_Prr site [Time series of CLM simulations (CLM\_PFT means changed surface vegetation, red lines; CLM\_Original means model default, blue lines) and observed surface soil temperature (black lines)]

表6 US\_Prr 站点 2012 年模拟表层土壤温度的评价指标

Table 6 Evaluation indexes of simulated surface soil temperature in 2012 at US\_Prr site

深度	模型	$R^2$	RMSE/°C	MAE/°C	MBE/°C
2 cm	CLM_Original	0.659	13.585	11.155	-5.452
	CLM_PFT	0.677	13.298	10.895	-5.978
5 cm	CLM_Original	0.576	13.546	11.094	-5.538
	CLM_PFT	0.592	13.311	10.931	-5.946

区苔原和针叶林站点, CLM5.0 在日尺度和月尺度都可以很好地模拟出 GPP 的时间变化特征, 其  $R^2$  均值为分别为 0.586 和 0.729。CLM5.0 虽然可以捕捉到 NEE 随时间的变化特征, 但是其模拟结果有一定的不确定性, 需要进一步对其参数化方案以及模型内在机理过程进行优化。CLM5.0 可以模拟出季节性 NEE 峰值时间, 虽然模型模拟的 NEE 峰值有轻微时间滞后, 但是也表明 CLM 可以扩展到区域分析区域碳循环。本研究可为 CLM5.0 在高纬度多年冻土区碳循环模拟的应用及改进提供一定的科学依据, 同时该研究结果对于理解北极地区的植被生长和碳循环对气候变化的响应具有重要意义。

### 参考文献 (References):

[1] Qin Dahe, Ding Yongjian, Xiao Cunde, et al. Cryospheric science: research framework and disciplinary system[J]. National Science Review, 2017, 5(2): 255-268.

[2] Hugelius G, Strauss J, Zubrzycki S, et al. Estimated stocks of circumpolar permafrost carbon with quantified uncertainty ranges and identified data gaps [J]. Biogeosciences, 2014, 11(23): 6573-6593.

[3] Schuur E A, McGuire A D, Schädel C, et al. Climate change and the permafrost carbon feedback [J]. Nature, 2015, 520(7546): 171-179.

[4] Strauss J, Schirrmeister L, Grosse G, et al. Deep Yedoma permafrost: a synthesis of depositional characteristics and carbon vulnerability[J]. Earth-Science Reviews, 2017, 172: 75-86.

[5] Schuur E A, Mack M C. Ecological response to permafrost thaw and consequences for local and global ecosystem services [J]. Annual Review of Ecology, Evolution, and Systematics, 2018, 49(1): 279-301.

[6] Huang Jianbin, Zhang Xiangdong, Zhang Qiyi, et al. Recently amplified arctic warming has contributed to a continual global warming trend [J]. Nature Climate Change, 2017, 7(12): 875-879.

[7] Biskaborn B K, Smith S L, Noetzi J, et al. Permafrost is warming at a global scale [J]. Nature Communications, 2019, 10(1): 264.

[8] Schädel C, Schuur E A, Bracho R, et al. Circumpolar assessment of permafrost C quality and its vulnerability over time using long-term incubation data [J]. Global Change Biology, 2014, 20(2): 641-652.

[9] Walker D A, Raynolds M K, Daniëls F J, et al. The circumpolar Arctic vegetation map [J]. Journal of Vegetation Science, 2005, 16(3): 267-282.

[10] Walker M D, Wahren C H, Hollister R D, et al. Plant community responses to experimental warming across the tundra biome [J]. Proceedings of the National Academy of Sciences of the United States of America, 2006, 103(5): 1342-1346.

[11] Myers-Smith I H, Kerby J T, Phoenix G K, et al. Complexity revealed in the greening of the Arctic [J]. Nature Climate Change, 2020, 10(2): 106-117.

[12] Soja A J, Tchekakova N M, French N H, et al. Climate-induced boreal forest change: predictions versus current observations [J]. Global and Planetary Change, 2007, 56(3/4): 274-296.

[13] Friedlingstein P, Jones M W, O'Sullivan M, et al. Global carbon budget 2021 [J]. Earth System Science Data, 2022, 14(4): 1917-2005.

[14] Koven C D, Ringeval B, Friedlingstein P, et al. Permafrost carbon-climate feedbacks accelerate global warming [J]. Proceedings of the National Academy of Sciences of the United States of America, 2011, 108(36): 14769-14774.

[15] McGuire A, Christensen T, Hayes D, et al. An assessment of the carbon balance of Arctic tundra: comparisons among obser-

- vations, process models, and atmospheric inversions[J]. *Biogeosciences*, 2012, 9(8): 3185-3204.
- [16] Arora V, Boer G. Terrestrial ecosystems response to future changes in climate and atmospheric CO<sub>2</sub> concentration[J]. *Biogeosciences*, 2014, 11(15): 4157-4171.
- [17] Ito A, Inatomi M, Huntzinger D N, et al. Decadal trends in the seasonal-cycle amplitude of terrestrial CO<sub>2</sub> exchange resulting from the ensemble of terrestrial biosphere models[J]. *Tellus B: Chemical and Physical Meteorology*, 2016, 68(1): 28968.
- [18] Danabasoglu G, Lamarque J, Bacmeister J, et al. The community earth system model version 2(CESM2)[J]. *Journal of Advances in Modeling Earth Systems*, 2020, 12(2): e2019MS001916.
- [19] Piao Shilong, Sitch S, Ciais P, et al. Evaluation of terrestrial carbon cycle models for their response to climate variability and to CO<sub>2</sub> trends[J]. *Global Change Biology*, 2013, 19(7): 2117-2132.
- [20] Lawrence D M, Slater A G, Swenson S C. Simulation of present-day and future permafrost and seasonally frozen ground conditions in CCSM4[J]. *Journal of Climate*, 2012, 25(7): 2207-2225.
- [21] Schädle C, Koven C D, Lawrence D M, et al. Divergent patterns of experimental and model-derived permafrost ecosystem carbon dynamics in response to Arctic warming[J]. *Environmental Research Letters*, 2018, 13(10): 105002.
- [22] Lawrence D M, Fisher R A, Koven C D, et al. The Community Land Model version 5: description of new features, benchmarking, and impact of forcing uncertainty[J]. *Journal of Advances in Modeling Earth Systems*, 2019, 11(12): 4245-4287.
- [23] Dos S T, Keppel-Aleks G, De Roo R, et al. Can land surface models capture the observed soil moisture control of water and carbon fluxes in temperate-to-boreal forests? [J]. *Journal of Geophysical Research: Biogeosciences*, 2021, 126(4): e2020JG005999.
- [24] Post H, Hendricks F H, Han Xujun, et al. Evaluation and uncertainty analysis of regional-scale CLM4.5 net carbon flux estimates[J]. *Biogeosciences*, 2018, 15(1): 187-208.
- [25] Wieder W R, Lawrence D M, Fisher R A, et al. Beyond static benchmarking: using experimental manipulations to evaluate land model assumptions[J]. *Global Biogeochemical Cycles*, 2019, 33(10): 1289-1309.
- [26] Umair M, Kim D, Ray R L, et al. Evaluation of atmospheric and terrestrial effects in the carbon cycle for forest and grassland ecosystems using a remote sensing and modeling approach[J]. *Agricultural and Forest Meteorology*, 2020, 295: 108187.
- [27] Birch L, Schwalm C R, Natali S, et al. Addressing biases in Arctic-boreal carbon cycling in the Community Land Model Version 5[J]. *Geoscientific Model Development*, 2021, 14(6): 3361-3382.
- [28] Jorgenson M, Yoshikawa K, Kanevskiy M, et al. Permafrost characteristics of Alaska in proceedings of the Ninth International Conference on Permafrost[DB]. Fairbanks, AK, USA: University of Alaska Fairbanks, 2008.
- [29] Jin Suming, Yang Limin, Zhu Zhe, et al. A land cover change detection and classification protocol for updating Alaska NLCD 2001 to 2011[J]. *Remote Sensing of Environment*, 2017, 195: 44-55.
- [30] Oechel W C, Laskowski C A, Burba G, et al. Annual patterns and budget of CO<sub>2</sub> flux in an Arctic tussock tundra ecosystem[J]. *Journal of Geophysical Research: Biogeosciences*, 2014, 119(3): 323-339.
- [31] Ikawa H, Nakai T, Busey R C, et al. Understory CO<sub>2</sub>, sensible heat, and latent heat fluxes in a black spruce forest in interior Alaska[J]. *Agricultural and Forest Meteorology*, 2015, 214: 80-90.
- [32] McEwing K R, Fisher J P, Zona D. Environmental and vegetation controls on the spatial variability of CH<sub>4</sub> emission from wet-sedge and tussock tundra ecosystems in the Arctic[J]. *Plant and Soil*, 2015, 388(1/2): 37-52.
- [33] Pastorello G, Trotta C, Canfora E, et al. The FLUXNET2015 dataset and the ONEFlux processing pipeline for eddy covariance data[J]. *Scientific Data*, 2020, 7(1): 225.
- [34] Naz B S, Kurtz W, Montzka C, et al. Improving soil moisture and runoff simulations at 3 km over Europe using land surface data assimilation[J]. *Hydrology and Earth System Sciences*, 2019, 23(1): 277-301.
- [35] Oleson K W, Lawrence D M, Gordon B, et al. Technical description of version 4.0 of the Community Land Model (CLM)[R]. Boulder, CO, USA: National Center for Atmospheric Research, 2010.
- [36] Lawrence D M, Oleson K W, Flanner M G, et al. Parameterization improvements and functional and structural advances in version 4 of the Community Land Model[J]. *Journal of Advances in Modeling Earth Systems*, 2011, 3(1): 2011MS00045.
- [37] Swenson S, Lawrence D M. Assessing a dry surface layer-based soil resistance parameterization for the Community Land Model using GRACE and FLUXNET-MTE data[J]. *Journal of Geophysical Research: Atmospheres*, 2014, 119(17): 10299-10312.
- [38] van Kampenhout L, Lenaerts J T, Lipscomb W H, et al. Improving the representation of polar snow and firn in the Community Earth System Model[J]. *Journal of Advances in Modeling Earth Systems*, 2017, 9(7): 2583-2600.
- [39] Medlyn B E, Duursma R A, Eamus D, et al. Reconciling the optimal and empirical approaches to modelling stomatal conductance[J]. *Global Change Biology*, 2011, 17(6): 2134-2144.
- [40] Ali A A, Xu Chonggang, Rogers A, et al. A global scale mechanistic model of photosynthetic capacity (LUNA V1.0)[J]. *Geoscientific Model Development*, 2016, 9(2): 587-606.
- [41] Ghimire B, Riley W J, Koven C D, et al. Representing leaf and root physiological traits in CLM improves global carbon and nitrogen cycling predictions[J]. *Journal of Advances in Modeling Earth Systems*, 2016, 8(2): 598-613.
- [42] Fisher J B, Sitch S, Malhi Y, et al. Carbon cost of plant nitrogen acquisition: a mechanistic, globally applicable model of plant nitrogen uptake, retranslocation, and fixation[J]. *Global Biogeochemical Cycles*, 2010, 24(1): 2009GB003621.
- [43] Brzostek E R, Fisher J B, Phillips R P. Modeling the carbon cost of plant nitrogen acquisition: mycorrhizal trade-offs and multipath resistance uptake improve predictions of retranslocation[J]. *Journal of Geophysical Research: Biogeosciences*, 2014, 119(8): 1684-1697.
- [44] Shi Mingjie, Fisher J B, Brzostek E R, et al. Carbon cost of plant nitrogen acquisition: global carbon cycle impact from an improved plant nitrogen cycle in the Community Land Model[J]. *Global Change Biology*, 2016, 22(3): 1299-1314.
- [45] Koven C D, Hugelius G, Lawrence D M, et al. Higher climatological temperature sensitivity of soil carbon in cold than warm climates[J]. *Nature Climate Change*, 2017, 7(11): 817-822.
- [46] Shangguan Wei, Dai Yongjiu, Duan Qingyun, et al. A global

- soil data set for earth system modeling[J]. *Journal of Advances in Modeling Earth Systems*, 2014, 6(1): 249-263.
- [47] Guo Donglin, Wang Huijun. Simulated change in the near-surface soil freeze/thaw cycle on the Tibetan Plateau from 1981 to 2010 [J]. *Chinese Science Bulletin*, 2014, 59 (20): 2439-2448.
- [48] Li Ren, Zhao Lin, Wu Tonghua, et al. Soil thermal conductivity and its influencing factors at the Tanggula permafrost region on the Qinghai-Tibet Plateau[J]. *Agricultural and Forest Meteorology*, 2019, 264: 235-246.
- [49] Yang Kai, Wang Chenghai, Li Shiyue. Improved simulation of frozen-thawing process in land surface model (CLM4.5) [J]. *Journal of Geophysical Research: Atmospheres*, 2018, 123 (23): 13238-13258.
- [50] Zheng Donghai, van der Velde R, Su Zhongbo, et al. Augmentations to the Noah model physics for application to the Yellow River source area. Part II: turbulent heat fluxes and soil heat transport [J]. *Journal of Hydrometeorology*, 2015, 16 (6): 2677-2694.
- [51] Yi Shuhua, McGuire A D, Harden J, et al. Interactions between soil thermal and hydrological dynamics in the response of Alaska ecosystems to fire disturbance[J]. *Journal of Geophysical Research: Biogeosciences*, 2009, 114 (G2): 2008JG000841.
- [52] Hinzman L D, Bettez N D, Bolton W R, et al. Evidence and implications of recent climate change in northern Alaska and other Arctic regions [J]. *Climatic Change*, 2005, 72 (3): 251-298.
- [53] Zhang Yinsheng, Munkhtsetseg E, Kadota T, et al. An observational study of ecohydrology of a sparse grassland at the edge of the Eurasian cryosphere in Mongolia [J]. *Journal of Geophysical Research: Atmospheres*, 2005, 110 (D14): 2004JD005474.
- [54] Shur Y L, Jorgenson M T. Patterns of permafrost formation and degradation in relation to climate and ecosystems [J]. *Permafrost and Periglacial Processes*, 2007, 18(1): 7-19.
- [55] Cox C J, Stone R S, Douglas D C, et al. Drivers and environmental responses to the changing annual snow cycle of northern Alaska [J]. *Bulletin of the American Meteorological Society*, 2017, 98(12): 2559-2577.
- [56] Toure A M, Rodell M, Yang Zongliang, et al. Evaluation of the snow simulations from the Community Land Model, version 4 (CLM4) [J]. *Journal of Hydrometeorology*, 2016, 17 (1): 153-170.
- [57] Hu Guojie, Zhao Lin, Zhu Xiaofan, et al. Review of algorithms and parameterizations to determine unfrozen water content in frozen soil [J]. *Geoderma*, 2020, 368: 114277.
- [58] Oleson K W, Niu G Y, Yang Z L, et al. Improvements to the Community Land Model and their impact on the hydrological cycle [J]. *Journal of Geophysical Research: Biogeosciences*, 2008, 113(G1): 2007JG000563.
- [59] Schaefer K, Zhang Tingjun, Slater A G, et al. Improving simulated soil temperatures and soil freeze/thaw at high-latitude regions in the Simple Biosphere / Carnegie-Ames-Stanford Approach model [J]. *Journal of Geophysical Research: Earth Surface*, 2009, 114(F2): 2008JF001125.
- [60] Yang Zongliang, Niu Guoyue, Mitchell K E, et al. The community Noah land surface model with multiparameterization options (Noah-MP): 2. evaluation over global river basins [J]. *Journal of Geophysical Research: Atmospheres*, 2011, 116 (D12): 2010JD015139.
- [61] Wang Chenghai, Yang Kai. A new scheme for considering soil water-heat transport coupling based on Community Land Model: model description and preliminary validation [J]. *Journal of Advances in Modeling Earth Systems*, 2018, 10(4): 927-950.
- [62] Seo H, Kim Y. Role of remotely sensed leaf area index assimilation in eco-hydrologic processes in different ecosystems over East Asia with Community Land Model version 4.5: biogeochemistry [J]. *Journal of Hydrology*, 2021, 594: 125957.
- [63] Cassidy A E, Christen A, Henry G H. Impacts of active retrogressive thaw slumps on vegetation, soil, and net ecosystem exchange of carbon dioxide in the Canadian High Arctic [J]. *Arctic Science*, 2017, 3(2): 179-202.
- [64] Bonan G B, Lawrence P J, Oleson K W, et al. Improving canopy processes in the Community Land Model version 4 (CLM4) using global flux fields empirically inferred from FLUXNET data [J]. *Journal of Geophysical Research: Biogeosciences*, 2011, 116(G2): 2010JG001593.
- [65] Hilton T W, Loik M E, Campbell J E. Simulating international drought experiment field observations using the community land model [J]. *Agricultural and Forest Meteorology*, 2019, 266: 173-183.
- [66] Bonan G B, Lombardozzi D L, Wieder W R, et al. Model structure and climate data uncertainty in historical simulations of the terrestrial carbon cycle (1850—2014) [J]. *Global Biogeochemical Cycles*, 2019, 33(10): 1310-1326.
- [67] Shirley I A, Mekonnen Z A, Grant R F, et al. Rapidly changing high-latitude seasonality: implications for the 21st century carbon cycle in Alaska [J]. *Environmental Research Letters*, 2022, 17(1): 014032.
- [68] Fisher J B, Sikka M, Oechel W C, et al. Carbon cycle uncertainty in the Alaskan Arctic [J]. *Biogeosciences*, 2014, 11 (15): 4271-4288.



## Applicability evaluation of CLM5.0 in simulating soil temperature and carbon cycle in Alaskan permafrost region

YAN Xuchun<sup>1,2</sup>, WU Xiaodong<sup>1</sup>, LÜ Yaqiong<sup>3</sup>, WU Tonghua<sup>1</sup>, LI Ren<sup>1</sup>, HU Guojie<sup>1</sup>,  
ZOU Defu<sup>1</sup>, LIU Yadong<sup>1,2</sup>, WEI Xianhua<sup>1,2</sup>, FAN Xiaoying<sup>1,2</sup>, WANG Dong<sup>1,2</sup>

(1. Cryosphere Research Station on the Qinghai-Tibet Plateau, State Key Laboratory of Cryospheric Science, Northwest Institute of  
Eco-Environment and Resources, Chinese Academy of Sciences, Lanzhou 730000, China; 2. University of Chinese  
Academy of Sciences, Beijing 100049, China; 3. Institute of Mountain Hazards and Environment,  
Chinese Academy of Sciences, Chengdu 610299, China)

**Abstract:** Climate warming has an important effect on Arctic permafrost and vegetation. Community Land Model (CLM) is one of the most widely used land surface models. However, the complex boundary conditions and parameterization process lead to uncertainty of the simulated results. In this study, we evaluated the simulation performance of the surface soil temperature and carbon cycle in Alaskan permafrost region using the CLM5.0. The results showed that CLM5.0 could capture the seasonal changes of surface soil temperature. At the tundra and needleleaf forests sites, the change of gross primary productivity (GPP) with time simulated by CLM5.0 on both daily and monthly scales were well simulated. The simulated net ecosystem exchange (NEE) has certain uncertainty. This study demonstrates that CLM5.0 can simulate the seasonal changes of soil temperature in high latitudinal permafrost region, but the model may be necessarily improved in the structure, parameterization scheme to improve the simulation accuracy for the carbon cycle.

**Key words:** CLM5.0; Alaska; soil temperature; carbon cycle; permafrost

(责任编辑: 赵林)